Inorg. Chem. **2005**, *44*, 1588–1600

Synthesis and Characterization of a Family of Structurally Characterized Dysprosium Alkoxides for Improved Fatigue-Resistance Characteristics of PDyZT Thin Films

Timothy J. Boyle,* Scott D. Bunge, Paul G. Clem, Jacob Richardson, Jeffrey T. Dawley, Leigh Anna M. Ottley, Mark A. Rodriguez, Bruce A. Tuttle, Gabriel R. Avilucea, and Ralph G. Tissot

Sandia National Laboratories, Advanced Materials Laboratory, 1001 University Boulevard SE, Albuquerque, New Mexico 87105

Received October 15, 2004

Using either an ammoniacal route, the reaction between $DyCl_3$, Na^0, and HOR in liquid ammonia, or preferentially reacting $Dy(N(SiMe_3)_2)_3$ with HOR in a solvent, we isolated a family of dysprosium alkoxides as $[Dy(\mu\text{-ONep})_2(ONep)]_4$ (**1**), $(ONep)_2Dy[(\mu_3\text{-ONep})(\mu\text{-ONep})Dy(ONep)(THF)]_2(\mu\text{-ONep})$ (**2**), $(ONep)_2Dy[(\mu_3\text{-ONep})(\mu\text{-ONep})Dy(ONep)(py)]_2(\mu\text{-ONep})$ (**3**), $[Dy_3(\mu_3\text{-OBu}^t)_2(\mu\text{-OBu}^t)_3(OBu^t)_4(HOBu^t)_2]$ (**4**), $[Dy_3(\mu_3\text{-OBu}^t)_2(\mu\text{-OBu}^t)_3(OBu^t)_4(THF)_2]$ (**5**), $[Dy_3(\mu_3\text{-OBu}^t)_2(\mu\text{-OBu}^t)_3(OBu^t)_4(py)_2]$ (**6**), $(DMP)Dy(\mu\text{-DMP})_4[Dy(DMP)_2(NH_3)]_2$ (**7**), $[Dy(\eta^6\text{-DMP})(DMP)_2]_2$ (**8**), $Dy(DMP)_3(THF)_3$ (**9**), $Dy(DMP)_3(py)_3$ (**10**), $Dy(DIP)_3(NH_3)_2$ (**11**), $[Dy(\eta^6\text{-DIP})(DIP)_2]_2$ (**12**), $Dy(DIP)_3(THF)_2$ (**13**), $Dy(DIP)_3(py)_3$ (**14**), $Dy(DBP)_3(NH_3)$ (**15**), $Dy(DBP)_3$ (**16**), $Dy(DBP)_3(THF)$ (**17**), $Dy(DBP)_3(py)_2$ (**18**), $[Dy(\mu\text{-TPS})(TPS)_2]_2$ (**19**), $Dy(TPS)_3(THF)_3$ (**20**), and $Dy(TPS)_3(py)_3$ (**21**), where ONep = OCH_2CMe_3, OBu^t = $OCMe_3$, DMP = $OC_6H_3(Me)_2$-2,6, DIP = $OC_6H_3(CHMe_2)_2$-2,6, DBP = $OC_6H_3(CMe_3)_2$-2,6, TPS = $OSi(C_6H_5)_3$, tol = toluene, THF = tetrahydrofuran, and py = pyridine. We were not able to obtain X-ray quality crystals of compounds **2**, **8**, and **9**. The structures observed and data collected for the Dy compounds are consistent with those reported for its other congeners. A number of these precursors were used as Dy dopants in $Pb(Zr_{0.3}Ti_{0.7})O_3$ (PZT 30/70) thin films, with compound **12** yielding the highest-quality films. The resulting $Pb_{0.94}Dy_{0.04}(Zr_{0.3}Ti_{0.7})O_3$ [PDyZT (4/30/70)] had similar properties to PZT (30/70), but showed substantial resistance to polarization reversal fatigue.

Introduction

Lead zirconium titanate (PZT), a solid solution of lead titanate and lead zirconate, is of current interest as a ferroelectric material for use in nonvolatile random-access memories in computers. One well-known disadvantage of this material is that it rapidly fatigues (10^5 cycles) when cycled on platinized silicon (Pt/Si) wafers. To overcome this problem, lanthanum (La^{3+}) is often added as a donor dopant for the A-site lead (Pb^{2+}) atoms. Although this works to minimize the fatigue, it also has the undesired effect of lowering the remanent polarization (P_r) of the resultant PLaZT.[1] Previously, we reported on the effects that the lanthanide series (Ln^{3+}) has on the polarization and dielectric constant (ϵ') when singularly doped into PZT, forming a series of PLnZT thin films.[1] From this study, we found that the aliovalent cations maintain the high polarization, yield square loops, and reduce fatigue on Pt/Si wafers. The aliovalent cations can, because of their size, occupy either or both the A- and B-site cations, acting as donor and acceptor dopants, respectively.

Initially, because of their commercial availability, the nitrate (NO_3) derivatives of the lanthanide series were used in the chemical solution route to these films. However, the NO_3 ligand has a rapid, large thermal decomposition pathway that can cause major disruption in the final thin film. As has been often reported, metal alkoxides are excellent precursors for solution routes to ceramic materials. It was surprising that there were only three structurally characterized dysprosium alkoxides $[Dy(OR)_3]$ reported in the literature: $Dy(OCH(CMe_3)_2)_3(NCMe)_2$,[2] $Dy(OC_5N(O\text{-}2))_3(H_2O)_2\cdot H_2O$,[3] and $[Dy(\mu\text{-OEtOMe})(OEtOMe)]_{10}$.[4] Therefore, we undertook the

* To whom correspondence should be addressed. Tel.: (505)272-7625. Fax: (505)272-7336. E-mail: tjboyle@Sandia.gov.

(1) Boyle, T. J.; Clem, P. G.; Tuttle, B. A.; Brennecka, G. L.; Dawley, J. T.; Rodriguez, M. A.; Dunbar, T. D.; Hammetter, W. F. *J. Mater. Res.* **2002** *17*, 871.

(2) Herrmann, W. A.; Anwander, R.; Scherer, W. *Chem. Ber.* **1993**, *126*, 1533.

10.1021/ic048550b CCC: $30.25
Published on Web 02/08/2005

synthesis and exploration of a series of systematically varied $Dy(OR)_3$ compounds as potential dopant precursors in PDyZT.

Several synthetic routes were undertaken in an attempt to generate this family of $Dy(OR)_3$ compounds and the products isolated proved by single-crystal X-ray diffraction to be **1** − **21** : $[Dy(\mu\text{-ONep})_2(ONep)]_4$ (**1**), $(ONep)_2Dy[(\mu_3\text{-ONep})(\mu\text{-ONep})Dy(ONep)(THF)]_2(\mu\text{-ONep})$ (**2**), $(ONep)_2Dy[(\mu_3\text{-ONep})(\mu\text{-ONep})Dy(ONep)(py)]_2(\mu\text{-ONep})$ (**3**), $[Dy_3(\mu_3\text{-OBu}^t)_2(\mu\text{-OBu}^t)_3(OBu^t)_4(HOBu^t)_2]$ (**4**), $[Dy_3(\mu_3\text{-OBu}^t)_2(\mu\text{-OBu}^t)_3(OBu^t)_4(THF)_2]$ (**5**), $[Dy_3(\mu_3\text{-OBu}^t)_2(\mu\text{-OBu}^t)_3(OBu^t)_4(py)_2]$ (**6**), $(DMP)Dy(\mu\text{-DMP})_4[Dy(DMP)_2(NH_3)]_2$ (**7**), $[Dy(\eta^6\text{-DMP})(DMP)_2]_2$ (**8**), $Dy(DMP)_3(THF)_3$ (**9**), $Dy(DMP)_3(py)_3$ (**10**), $Dy(DIP)_3(NH_3)_2$ (**11**), $[Dy(\eta^6\text{-DIP})(DIP)_2]_2$ (**12**), $Dy(DIP)_3(THF)_2$ (**13**), $Dy(DIP)_3(py)_3$ (**14**), $Dy(DBP)_3(NH_3)$ (**15**), $Dy(DBP)_3$ (**16**), $Dy(DBP)_3(THF)$ (**17**), $Dy(DBP)_3(py)_2$ (**18**), $[Dy(\mu\text{-TPS})(TPS)_2]_2$ (**19**), $Dy(TPS)_3(THF)_3$ (**20**), and $Dy(TPS)_3(py)_3$ (**21**), where ONep = *neo*-pentoxide (OCH_2CMe_3), OBu^t = *tert*-butoxide ($OCMe_3$), DMP = 2,6-dimethyl phenoxide [$OC_6H_3(Me)_2$-2,6], DIP = 2,6-diisopropyl phenoxide [$OC_6H_3(CHMe_2)_2$-2,6], DBP = 2,6-di-*tert*-butyl phenoxide [$OC_6H_3(CMe_3)_2$-2,6], TPS = triphenylsiloxide [$OSi(C_6H_5)_3$], tol = toluene, THF = tetrahdyrodfuran, and py = pyridine.

Figures 1−20 are plots of **1**−**21** (note that X-ray quality crystals of compounds **2**, **8**, and **9** were not isolated). Selected representative species from this family of compounds were used as aliovalent dopant precursors in PDyZT thin films. The ferroelectric properties of the final ceramic PDyZT thin films characterized during this study are also reported.

Experimental Section

All compounds described below were handled with rigorous exclusion of air and water using standard Schlenk-line and glovebox techniques. All solvents were stored under argon and used as received (Aldrich) in sure-seal bottles, including hexanes (hex), tol, THF, and py. The following chemicals were used as received (Aldrich): $DyCl_3$, Na^0, $LiN(SiMe_3)_2$ ($LiNR_2$), H−ONep, H−OBu^t, H−DMP, H−DIP, H−DBP, and H−TPS. NH_3(g) was used as received (Tri-gas, Inc.).

FT-IR data were obtained on a Bruker Vector 22 Instrument using KBr pellets under an atmosphere of flowing nitrogen. Elemental analysis was performed on a Perkin-Elmer 2400 CHN−S/O elemental analyzer.

General Syntheses. (a) Ammoniacal. Following the ammoniacal preparative route reported by Clark and co-workers for $La(OAr)_3$ species,[5] $DyCl_3$ was reacted with 3 equiv of Na^0 in NH_3(l) at −78 °C, followed by addition of 3 equiv of the desired HOR dissolved in tol (eq 1, Results and Discussion). From the powder isolated after the mixture was warmed to room temperature, crystals of the NH_3 adducts were isolated by dissolution in tol and cooling to −35 °C. NH_3-free species were isolated by refluxing of the powder redissolved in tol, followed by drastic reduction of the volatile portion of the reaction mixture and then cooling to −35 °C or slow evaporation in a glovebox. THF and py adducts were isolated by redissolution of the NH_3 adduct or the NH_3-free adduct in the appropriate solvent, followed by crystallization at low temperature (−35 °C) or slow evaporation under an argon atmosphere.

(b) Amide. $DyCl_3$ was reacted with 3 equiv of $LiNR_2$ in diethyl ether (Et_2O), and the resultant precipitate was removed by centrifugation (eq 2, Results and Discussion). The resulting pale yellow powder was washed several times with hex, sublimed, crystallized, and then used without further purification. X-ray quality crystals were grown from hexanes and proved to be $Dy(NR_2)_3$, which was isostructural with literature reports.[6] The pure $Dy(NR_2)_3$ was reacted with the desired HOR in the respective solvent to isolate the various species of interest (eq 3, Results and Discussion). Crystals were grown by slow evaporation or cooling of the reaction mixture to −35 °C. Yields were not optimized.

$[Dy(\mu\text{-ONep})_2(ONep)]_4$ (1). The synthesis used $Dy(NR_2)_3$ (2.0 g, 3.1 mmol) and HONep (0.96 g, 10.9 mmol) in 5 mL of tol. Yield 0.84 g (60%). FT-IR (KBr, cm^{-1}): 2953 (s), 2866 (s), 2811 (s), 2741 (m), 2696 (w), 1655 (m, br), 1611 (w), 1608 (w), 1560 (m), 1508 (s), 1479 (m), 1464 (m), 1411 (w), 1393 (m), 1364 (m), 1329 (w), 1259 (w), 1217 (w), 1125 (s), 1066 (m), 1039 (m), 1020 (m), 934 (w), 898 (w), 752 (w), 607 (w), 568 (w), 468 (w), 417 (w). Elemental analysis for $C_{60}H_{132}Dy_4O_{12}$: Calcd 42.50% C, 7.84% H. Found 41.87% C, 7.66% H.

$Dy_3(\mu_3\text{-ONep})_2(\mu\text{-ONep})_3(ONep)_4(py)_2$ (3). The synthesis used $Dy(NR_2)_3$ (1.0 g, 1.6 mmol) and HONep (0.48 g, 5.4 mmol) in 5 mL of py. Yield 0.52 g (67%). FT-IR (KBr, cm^{-1}): 2952 (s), 2903 (m), 2865 (m), 2808 (m), 2692 (w), 1603 (m), 1479 (m), 1460 (m), 1445 (m), 1393 (m), 1360 (m), 1259 (w), 1219 (w), 1128 (s), 1060 (s), 1020 (s), 935 (w), 898 (w), 751 (w), 704 (w), 602 (w), 569 (w), 417 (w). Elemental analysis for $C_{115}H_{238}Dy_6N_5O_{18}$: Calcd 46.75% C, 8.12% H, 2.37% N. Found 47.85% C, 7.20% H, 2.78% N.

$Dy_3(\mu_3\text{-OBu}^t)_2(\mu\text{-OBu}^t)_3(OBu^t)_4(HOBu^t)_2$ (4). The synthesis used $Dy(NR_2)_3$ (1.0 g, 1.6 mmol) and $HOBu^t$ (0.40 g, 5.4 mmol) in 5 mL of tol. Yield 0.42 g (63%). FT-IR (KBr, cm^{-1}): 3440 (br), 2962 (s), 2922 (m), 2896 (m), 2863 (m), 1474 (w), 1459 (w), 1379 (m), 1357 (m), 1206 (s), 1007 (m), 942 (m), 902 (m), 762 (w), 528 (m, br), 475 (m). Elemental analysis for $C_{44}H_{101}Dy_3O_{11}$: Calcd 40.84% C, 7.86. Found 40.67% C, 7.11% H.

$Dy_3(\mu_3\text{-OBu}^t)_2(\mu\text{-OBu}^t)_3(OBu^t)_4(THF)_2$ (5). The synthesis used $Dy(NR_2)_3$ (0.25 g, 0.39 mmol) and $HOBu^t$ (0.10 g, 1.4 mmol) in 5 mL of THF. Yield 0.65 g (71%). FT-IR (KBr, cm^{-1}): 3448 (br), 2969 (s), 2928 (m), 2901 (m), 2863 (m), 1473 (m), 1467 (m), 1381 (m), 1371 (m), 1357 (m), 1240 (m), 1203 (s), 1181 (s), 1164 (m), 991 (s), 983 (s), 935 (s), 902 (s),879 (m), 764 (m), 741 (m), 5278 (m), 493 (m), 476 (m). Elemental analysis for $C_{44}H_{97}Dy_3O_{11}$: Calcd 40.97% C, 7.58, % H. Found 40.73% C, 7.69% H.

$Dy_3(\mu_3\text{-OBu}^t)_2(\mu\text{-OBu}^t)_3(OBu^t)_4(py)_2$ (6). The synthesis used $Dy(NR_2)_3$ (1.0 g, 1.6 mmol) and $HOBu^t$ (0.40 g, 5.4 mmol) in 5 mL of py. Yield 0.37 g (56%). FT-IR (KBr, cm^{-1}): 2966 (s), 2924 (m), 2900 (m), 2868 (m), 1601 (w), 1442 (m), 1371 (m), 1355 (m), 1199 (s), 999 (s), 991 (s), 993 (s) 903 (m), 763 (m), 751 (m), 700 (s), 615 (w), 524 (m), 492 (m), 476 (m), 403 (w). Elemental analysis for $C_{46}H_{91}Dy_3N_2O_9$: Calcd 42.38% C, 7.04% H, 2.15% N. Found 41.19% C, 6.75% H, 1.59% N.

$Dy_3(\mu\text{-DMP})_4(DMP)_5(NH_3)_2$ (7). The synthesis used $DyCl_3$ (2.5 g, 9.2 mmol), Na^0 (0.64 g, 27.8 mmol), and H−DMP (3.9 g, 32 mmol) in 20 mL of tol. Yield 3.89 g (73.6%). FT-IR (KBr, cm^{-1}): 3358 (w), 3282 (w), 3057 (w), 3024 (w), 2960 (s), 2960 (m), 2927 (m), 2868 (m), 1588 (w), 1458 (m), 1430 (s), 1382 (w), 1358 (w),

(3) Tesdeschi, C.; Azema, J.; Gornitzka, H.; Tisnes, P.; Picard, C. *Dalton Trans.* **2003**,1738.
(4) Westin, L. C.; Kritikox, M.; Caneschi, A. *Chem. Commun.* **2003**, 1012.
(5) Butcher, R. J.; Clark, D. L.; Grumbine, S. K.; Vincent-Hollis, R. L.; Scott, B. L.; Watkin, J. G. *Inorg. Chem.* **1995**, *34*, 5468.
(6) Hermmann, W. A.; Anwander, R.; Munck, F. C.; Scherer, W.; Dufaud, V.; Huber, N. W.; Artus, G. R. J. *Z. Naturforsch. B* **1994**, *49*, 1789.

1332 (m), 1272 (s), 1208 (s), 1172 (w), 1147 (w), 1109 (w), 1042 (m), 931 (w), 887 (m), 862 (m), 824 (w), 803 (w), 793 (m), 748 (m), 731 (w), 689 (m), 614 (w), 568 (m), 556 (m), 467 (w). Elemental analysis for $C_{79}H_{95}Dy_3N_2O_9$: Calcd 55.68% C, 5.62% H, 1.64% N. Found 56.33% C, 5.95% H, 1.58% N.

[Dy(η^6-DMP)(DMP)$_2$]$_2$ (8). The synthesis used $Dy(NR_2)_3$ (0.25 g, 0.39 mmol) and H−DMP (0.17 g, 1.4 mmol) in 5 mL of tol. Yield 0.45 g (55%). FT-IR (KBr, cm^{-1}): 2969 (s), 2928 (m), 2901 (m), 2869 (m), 1467 (m), 1381 (m), 1371 (m), 1357 (m), 1240 (m), 1203 (s), 1181 (s), 1165 (m), 991 (s), 982 (s), 935 (s), 902 (s), 877 (m), 768 (m), 743 (m), 528 (m), 494 (m), 476 (m). Elemental analysis for $C_{24}H_{27}DyO_3$: Calcd 54.80% C, 7.49% H. Found 55.87% C,5.98% H.

Dy(DMP)$_3$(THF)$_3$ (9). The synthesis used $Dy(NR_2)_3$ (0.25 g, 0.39 mmol) and H−DMP (0.17 g, 1.4 mmol) in 5 mL of THF. Yield 0.23 g (32%). FT-IR (KBr, cm^{-1}): 3068 (w), 3039 (w), 2958 (s), 2922 (s), 2854 (m), 1592 (m), 1564 (m), 1544 (w), 1516 (w), 1467 (s), 1450 (s), 1439 (s), 1428 (s), 1389 (w), 1381 (w), 1287 (s), 1265 (s), 1222 (m), 1092 (s), 916 (m), 848 (m), 803 (m), 760 (m), 704 (m). Elemental analysis for $C_{36}H_{51}DyO_6$: Calcd 58.00% C, 6.93% H. Found 49.01% C, 5.21% H.

Dy(DMP)$_3$(py)$_3$ (10). The synthesis used $Dy(NR_2)_3$ (1.0 g, 1.6 mmol) and H−DMP (0.67 g, 5.4 mmol) in 5 mL of py. Yield 0.20 g (24%). FT-IR (KBr, cm^{-1}): 3135 (w), 3067 (w), 3035 (w), 3012 (w), 2959 (m), 2924 (s), 2854 (m), 2723 (w), 1597 (s), 1591 (s), 1572 (m), 1531 (m), 1545 (m), 1510 (m), 1476 (s), 1466 (s), 1442 (s), 1425 (s), 1342 (m), 1286 (s), 1242 (m), 1217 (m), 1155 (w), 1090 (s), 1069 (m), 1037 (s), 1004 (m), 991 (w), 915 (w) 873 (s), 858 (s), 804 (w), 756 (s), 748 (s), 703 (s), 622 (m), 603 (w), 562 (w), 533 (s), 488 (w), 469 (w), 415 (w), 407 (m). Elemental analysis for $C_{88}H_{94}Dy_2N_8O_6$: Calcd 62.73% C, 5.62% H, 6.65% N. Found 62.08% C, 5.82% H, 6.15% N.

Dy(DIP)$_3$(NH$_3$)$_2$ (11). The synthesis used $DyCl_3$ (5.0 g, 18 mmol), Na^0 (1.3 g, 568 mmol), and H−DIP (3.3 g, 64 mmol) in 40 mL of tol. Yield 6.6 g (57%). FT-IR (KBR, cm^{-1}): 2961 (s), 2914 (m), 2866 (m), 1589 (w), 1461 (m), 1431 (s), 1383 (w), 1360 (w), 1331 (m), 1273 (m), 1207 (m), 1146 (w), 1111 (w), 1043 (w), 888 (m), 862 (m), 793 (w), 762 (w), 748 (m). Elemental analysis for $C_{27}H_{57}DyN_2O_3$: Calcd 52.35% C, 9.27% H, 4.52% N. Found 59.47% C, 7.82% H, 3.10% N.

[Dy(η^6-DIP)(DIP)$_2$]$_2$ (12). The synthesis used $Dy(NR_2)_3$ (1.0 g, 1.6 mmol) and H−DIP (0.97 g, 5.4 mmol) in 5 mL of tol. Yield 0.71 g (33%). FT-IR (KBr, cm^{-1}): 3367 (m), 3278 (w), 3055 (m), 3024 (w), 2960 (s), 2928 (m), 2867 (m), 1589 (m), 1459 (m), 1433 (s),1383 (m), 1360 (m), 1328 (s), 1267 (s), 1202 (s), 1182 (s), 1157 (w), 1146 (w), 1103 (s), 887 (s), 861 (s), 829 (m), 797 (m) 753 (s), 733 (m), 696 (m), 619 (w), 598 (w), 572 (m), 545 (m), 466 (w), 453 (w), 426 (m). Elemental analysis for $C_{72}H_{102}Dy_2O_6$: Calcd 62.28% C, 7.40% H. Found 62.42% C, 7.25% H.

Dy(DIP)$_3$(THF)$_2$ (13). The synthesis used $Dy(NR_2)_3$ (1.0 g, 1.6 mmol) and H−DIP (0.97 g, 5.4 mmol) in 5 mL of THF. Yield 0.33 g (26%). FT-IR (KBr, cm^{-1}): 2960 (s), 2893 (m), 2863 (m), 1588 (m), 1461 (m), 1431 (s), 1381 (m), 1358 (m), 1331 (s), 1273 (s), 1210 (s), 111 (w), 1095 (w), 1042 (m), 1017 (m), 888 (s), 863 (s), 755 (s), 691 (m), 564 (m). Elemental analysis for $C_{44}H_{67}DyO_5$: Calcd 63.03% C, 8.05% H. Found 62.70% C, 8.35% H.

Dy(DIP)$_3$(py)$_3$ (14). The synthesis used $Dy(NR_2)_3$ (1.0 g, 1.6 mmol) and H−DIP (0.97 g, 5.4 mmol) in 5 mL of py. Yield 0.53 g (34%). FT-IR (KBr, cm^{-1}): 3064 (w), 2966 (s), 2955 (m), 2865 (m), 1597 (m), 1462 (w), 1443 (s), 1430 (s), 1380 (w), 1332 (s), 1270 (s), 1213 (s), 1154 (m), 1070 (w), 1037 (w), 1002 (w), 888 (m), 859 (m), 751 (s), 705 (s). Elemental analysis for $C_{56}H_{71}DyN_4O_3$: Calcd 66.50% C, 7.08% H, 5.54% N. Found 66.20% C, 7.05% H, 5.92% N.

Dy(DBP)$_3$(NH$_3$) (15). The synthesis used $DyCl_3$ (2.5 g, 9.3 mmol), Na^0 (0.64, 28 mmol), and H−DBP (6.7 g, 33 mmol) in 40 mL of tol. Yield 3.5 g (52%). Elemental analysis for $C_{42}H_{66}DyNO_3$: Calcd 63.42% C, 8.36% H, 1.76% N. Found 66.47% C, 8.27% H, 0.5% N.

Dy(DBP)$_3$ (16). The synthesis used $Dy(NR_2)_3$ (5.0 g, 7.8 mmol) and H−DBP (2.4 g, 27.2 mmol) in 20 mL of tol. Yield 6.1 g (50.4%). FT-IR (KBr, cm^{-1}): 3646 (s), 3080 (m), 2957 (s), 2916 (s), 2872 (s), 1584 (m), 1478 (m), 1458 (s), 1425 (s), 1411 (m), 1387 (m), 1359 (m), 1309 (m) 1249 (s, br), 1196 (m), 1176 (m), 1144 (m), 1121 (m) 1098 (m), 1019 (w), 956 (w), 873 (s), 842 (m), 819 (m), 808 (m), 794 (m), 747 (s), 663 (s), 589 (m), 549 (m), 523 (w), 449 (m). Elemental analysis for $C_{84}H_{126}Dy_2O_6$: Calcd 64.81% C, 8.16% H. Found 38.97% C, 5.28% H.

Dy(DBP)$_3$(THF) (17). The synthesis used $Dy(NR_2)_3$ (1.0 g, 1.6 mmol) and H−DBP (1.1 g, 5.4 mmol) in 5 mL of THF. Yield 0.30 g (23%). FT-IR (KBr, cm^{-1}): 3081 (w), 3059 (w), 3003 (m) 2958 (s), 2919 (m), 2873 (m), 1476 (m), 1459 (m), 1426 (s), 1408 (s), 1388 (m), 1362 (m), 1314 (m), 1260 (s), 1248 (s), 1232 (s), 1199 (m), 1172 (m), 1141 (m), 1123 (m), 1106 (m), 1094 (m), 955 (w), 928 (w), 864 (m), 845 (m), 822 (m), 806 (m), 794 (m), 747 (s), 969 (m), 666 (w), 954 (m), 588 (w), 542 (m), 529 (w), 446 (w), 418 (w). Elemental analysis for $C_{46}H_{71}DyO_4$: Calcd 64.96% C, 8.41% H. Found 65.68% C, 8.27% H.

Dy(DBP)$_3$(py)$_2$ (18). The synthesis used $Dy(NR_2)_3$ (1.0 g, 1.6 mmol) and H−DBP (1.1 g, 5.4 mmol) in 5 mL of py. Yield 0.15 g (11.3%). FT-IR (KBr, cm^{-1}): 3080 (w), 3049 (w), 3002 (w, sh), 2958 (s), 2922 (m), 2871 (m), 1405 (s), 1261 (s), 1258 (s), 1229 (s), 1199 (m), 1101 (m), 1070 (m), 1041 (m), 1008 (m), 884 (w), 864 (s), 856 (s), 816 (s), 807 (s), 797 (s), 751 (s), 709 (s), 656 (m), 643 (m), 626 (m), 610 (m), 546 (w), 466 (w). Elemental analysis for $C_{52}H_{73}DyN_2O_3$: Calcd 66.68% C, 7.86% H, 2.99% N. Found 67.08% C, 7.63, % H, 2.86% N.

[Dy(μ-TPS)(TPS)$_2$]$_2$ (19). The synthesis used $Dy(NR_2)_3$ (0.23 g, 0.36 mmol), TPS−H (0.3, 1.1 mmol) in 5 mL of tol. Yield 0.19 g (51%). FT-IR (KBr, cm^{-1}): 3066 (s), 3049 (m), 3016 (m), 2963 (m), 2930 (m) 1261 (w), 1185 (w), 1158 (w), 1113 (s), 1067 (w), 1046 (w), 1035 (m), 1000 (m), 979 (m), 869 (w), 835 (w), 744 (m), 702 (s), 672 (w), 517 (s). Elemental analysis for $C_{115}H_{98}Dy_2O_6Si_6$: Calcd 66.74% C, 4.77% H. Found 66.82% C, 5.34% H.

Dy(TPS)$_3$(THF)$_3$ (20). The synthesis used $Dy(NR_2)_3$ (0.23 g, 0.36 mmol), TPS−H (0.3, 1.1 mmol) in 5 mL of THF. Yield 0.39 g (87%). FT-IR (KBr, cm^{-1}): 3066 (s), 3049 (s), 3016 (m), 2963 (w), 2930 (w), 1433 (s), 1263 (m), 1187 (m), 1116 (s), 1068 (m), 1042 (w), 1028 (w), 1000 (m), 978 (s), 860 (m), 837 (w), 738 (m), 703 (s), 671 (m), 517 (s). Elemental analysis for $C_{70}H_{77}DyO_7Si_3$: Calcd 65.83% C, 6.07% H. Found 65.74% C, 5.98% H.

Dy(TPS)$_3$(py)$_3$ (21). The synthesis used $Dy(NR_2)_3$ (0.23 g, 0.36 mmol), TPS−H (0.3, 1.1 mmol) in 5 mL of py. Yield 0.23 g (52%). FT-IR (KBr, cm^{-1}): 3062 (w), 3064 (s), 3044 (s), 3020 (m), 3006 (m), 2996 (m), 2963 (m), 2927 (m), 1599 (m), 1536 (w), 1482 (w), 1441 (s), 1427 (s), 1378 (w), 1262 (w), 1215 (w), 1186 (w), 1151 (w), 1109 (s), 1062 (m), 1033 (m), 1024 (m), 999 (m), 980 (s), 714 (m), 701 (s), 618 (w), 518 (s). Elemental analysis for $C_{69}H_{60}DyN_3O_3Si_3$: Calcd 67.60% C, 4.93% H, 3.43% N. Found 67.12% C, 5.08% H, 3.80% N.

General X-ray Crystal Structure Information.[7] Each crystal was mounted onto a thin glass fiber from a pool of Fluorolube and immediately placed under a liquid N_2 stream on a Bruker AXS diffractometer. The radiation used was graphite monochromatized

Table 1. Data Collection Parameters for **1**, **1a**, and **3**

	1	**1a**	**3**
chemical formula	$C_{67}H_{140}Dy_4O_{12}$	$C_aH_bDy_cNa_dO_e$	$C_{115}H_{238}Dy_6N_5O_{18}$
formula weight	1787.79	−	2954.10
temp (K)	293(2)	223(2)	168(2)
space group	tetragonal	tetragonal	monoclinic
	$P\bar{4}2(1)c$	$I4/m$	$C2/c$
a (Å)	20.324(5)	15.002(2)	17.4909(17)
b(Å)	20.324(5)	15.002(2)	22.228(2)
c (Å)	11.976(4)	19.733(4)	18.1697(18)
β (deg)			94.911(2)
V (Å^3)	4947(2)	4440.8(11)	7038.3(12)
Z	2	−	2
D_{calcd} (Mg/m^3)	1.200	−	1.394
μ (Mo Kα) (mm^{-1})	3.026	4.221	3.198
R1[a] (%) (all data)	2.64 (3.16)	9.89 (14.73)	6.11 (8.96)
wR2[b] (%) (all data)	7.19 (7.35)	27.73 (30.82)	15.64 (17.02)

[a] $R1 = \sum||F_o| - |F_c||/\sum |F_o|$ x 100. [b] $wR2 = [\sum w(F_o^2 - F_c^2)^2/\sum(w|F_o|^2)^2]^{1/2}$ x 100.

Mo Kα radiation (λ = 0.7107 Å). The lattice parameters were optimized from a least-squares calculation on carefully centered reflections. Lattice determination and data collection were carried out using SMART version 5.054 software. Data reduction was performed using SAINT version 6.01 software. The structure refinement was performed using XSHELL 3.0 software. The data were corrected for absorption using the SADABS program within the SAINT software package.

Each structure was solved using direct methods. This procedure yielded the heavy atoms, along with a number of the C, N, and O atoms. Subsequent Fourier synthesis yielded the remaining atom positions. The hydrogen atoms were fixed in positions of ideal geometry and refined within the XSHELL software. These idealized hydrogen atoms had their isotropic temperature factors fixed at 1.2 or 1.5 times the equivalent isotropic U value of the C atoms to which they were bonded. The final refinement of each compound included anisotropic thermal parameters on all non-hydrogen atoms. Additional information concerning the data collection and final structural solutions of **1**−**21** can be found in the Supporting Information. Any variations from standard structural solution associated with the representative compounds, are discussed below. Data collection parameters are listed in Tables 1−6.

Film Production. Standard spin-coat deposition routes[8] were used to generate the PDyZT thin films. A brief description of the preparation and processing follows. The PZT (30/70) films were produced following the established BRP route,[8,9] in which $Pb(O_2CCH_3)_2{\cdot}(HO_2CCH_3)$ (Aldrich, 95%) dissolved in pyridine (py) was added to a mixture of $Ti(OCH(CH_3)_2)_4$ (Aldrich, distilled) and $[Zr(OCH(CH_3)_2)_4(HOCH(CH_3)_2)]_2$ (Aldrich) dissolved in tol to form the PZT precursor mixture. Compound **12** was dissolved in py and then added to the PZT mixture to form the ∼0.4 M PDyZT precursor solution.

Multilayered films of the desired composition were spin-coat deposited, in air, onto Pt(1700 Å)/Ti(300 Å)-coated, thermally oxidized SiO_2/Si substrates using a photoresist spinner (3000 rpm for 30 s). After each deposition, the films were heated on a hot plate (300 °C for ∼5 min) and allowed to cool to room temperature before the deposition of the next layer. After the final layer received the 300 °C treatment (for this study, 2−4 layers were used), the film was crystallized in a tube furnace at 650 °C for 30 min in air.

(7) The listed versions of SAINT, SMART, XSHELL, XPOW in SHELXTL, and SADABS Software from Bruker Analytical X-ray Systems Inc., 6300 Enterprise Lane, Madison, WI 53719, were used in analysis.

(8) Boyle, T. J.; Al-Shareef, H. N. *J. Mater. Sci.* **1997**, *32*, 2263.
(9) Boyle, T. J. U.S. Patent 5,858,451, 1991.

Table 2. Data Collection Parameters for **4**−**6**

	4	**5**	**6**
chemical formula	$C_{44}H_{101}Dy_3O_{11}$	$C_{44}H_{97}Dy_3O_{11}$	$C_{46}H_{91}Dy_3N_2O_9$
formula weight	1293.75	1289.72	1303.74
temp (K)	168(2)	203(2)	203(2)
space group	monoclinic	orthorhombic	monoclinic
	$P2(1)/c$	$Pbcn$	$C2/c$
a (Å)	19.369(2)	13.8708(17)	17.188(2)
b(Å)	10.7734(13)	19.8030(19)	19.665(2)
c (Å)	27.295(3)	17.6311(18)	17.630(2)
α (deg)			
β (deg)	99.308(2)		90.257(2)
γ (deg)			
V (Å^3)	5620.8(12)	5890.4(10)	5959.1(13)
Z	4	4	−
D_{calcd} (Mg/m^3)	1.529	1.546	−
μ (Mo Kα) (mm^{-1})	3.994	3.817	5.025
R1[a] (%) (all data)	3.98 (5.03)	5.83 (8.17)	11.55 (12.72)
wR2[b] (%) (all data)	7.93 (8.43)	12.18 (13.18)	33.12 (34.30)

[a] $R1 = \sum||F_o| - |F_c||/\sum|F_o|$ x 100. [b] $wR2 = [\sum w(F_o^2 - F_c^2)^2/\sum(w|F_o|^2)^2]^{1/2}$ x 100.

Table 3. Data Collection Parameters for **7** and **10**

	7	**10**
chemical formula	$C_{79}H_{95}Dy_3N_2O_9$	$C_{88}H_{94}Dy_2N_8O_6$
formula weight	1704.07	1684.71
temp (K)	223(2)	168(2)
space group	monoclinic	triclinic
	$P2(1)$	$P\bar{1}$
a (Å)	11.758(2)	10.712(15)
b(Å)	22.320(4)	13.799(20)
c (Å)	14.171(3)	27.84(4)
α (deg)		81.94(2)
β (deg)	94.503(4)	87.51(2)
γ (deg)		74.07(2)
V (Å^3)	3707.6(11)	3918(9)
Z	2	2
D_{calcd} (Mg/m^3)	1.526	1.428
μ (Mo Kα) (mm^{-1})	3.048	1.951
R1[a] (%) (all data)	9.63 (18.32)	6.29 (12.82)
wR2[b] (%) (all data)	14.85 (18.06)	9.87 (13.97)

[a] $R1 = \sum||F_o| - |F_c||/\sum|F_o|$ x 100. [b] $wR2 = [\sum w(F_o^2 - F_c^2)^2/\sum(w|F_o|^2)^2]^{1/2}$ x 100.

X-ray diffraction (XRD) was used to confirm the phase purity and orientation of the final films.

Ferroelectric Testing. To measure the electrical properties of the films, gold top electrodes (∼250 × 250 μm) were sputter-deposited onto the films using a shadow mask to create a parallel-plate capacitor geometry. Capacitor top electrode areas were individually measured with a calibrated optical microscope, and film thicknesses were measured using a Dektak profilometer. The low-field dielectric properties were measured at 10 kHz (100 mV p−p) using an HP 4284A impedance analyzer (Palo Alto, CA). The ferroelectric properties of the PLnZT films were measured using an RT66A ferroelectric tester from Radiant Technologies (Albuquerque, NM). Accelerated ferroelectric fatigue tests were performed using a 1-MHz bipolar square-wave pulse, with the applied electric field normalized to ∼700 kV/cm.

Results and Discussion

Because of our interest in doping PZT with aliovalent lanthanide cations coupled with the dearth of readily available acceptable Dy precursors, it was necessary to develop a family of $Dy(OR)_3$ compounds. As mentioned previously, the nitrate derivatives, though convenient because they are commercially available, do not always generate the highest-

Table 4. Data Collection Parameters for **11**−**14**

	11	**12**	**13**	**14**
chemical formula	$C_{27}H_{38.50}DyN_2O_3$	$C_{72}H_{102}Dy_2O_6$	$C_{44}H_{67}DyO_5$	$C_{56}H_{71}DyN_4O_3$
formula weight	601.60	1388.54	838.48	1010.67
temp (K)	168(2)	223(2)	168(2)	162(2)
space group	triclinic	monoclinic	monoclinic	monoclinic
	$P\bar{1}$	$P2(1)/c$	$P2(1)$	Cc
a (Å)	15.671(4)	17.105(18)	9.7320(13)	18.503(3)
b(Å)	20.199(6)	21.56(2)	19.330(3)	18.032(2)
c (Å)	29.257(8)	9.669(10)	12.1195(16)	15.808(2)
α (deg)	105.495(4)			
β (deg)	91.344(5)	105.84(2)	109.628(2)	96.811(2)
γ (deg)	111.208(4)			
V (Å^3)	8245(4)	3430(6)	2147.4(5)	5237.3(12)
Z	8	2	2	4
D_{calcd} (Mg/m^3)	0.969	1.344	1.297	1.282
μ (Mo Kα) (mm^{-1})	1.831	2.209	1.780	1.471
R1[a] (%) (all data)	8.26 (13.29)	7.02 (12.69)	2.34 (4.93)	4.93 (6.01)
wR2[b] (%) (all data)	22.69 (25.04)	14.53 (17.17	2.80 (5.07)	9.98 (10.35)

[a] $R1 = \sum||F_o| - |F_c||/\sum |F_o|$ x 100. [b] $wR2 = [\sum w(F_o^2 - F_c^2)^2/\sum(w|F_o|^2)^2]^{1/2}$ x 100.

Table 5. Data Collection Parameters for **15**−**18**

	15	**16**	**17**	**18**
chemical formula	$C_{42}H_{66}DyNO_3$	$C_{84}H_{126}Dy_2O_6$	$C_{46}H_{71}DyO_4$	$C_{52}H_{73}DyN_2O_3$
formula weight	795.46	1556.85	850.53	936.62
temp (K)	168(2)	168(2)	168(2)	178(2)
space group	monoclinic	monoclinic	orthorhombic	orthorhombic
	$P2(1)/n$	$P2(1)$	*Pbca*	*Pbcn*
a (Å)	12.5879(12)	11.2323(8)	20.130(6)	20.474(2)
b(Å)	14.6871(14)	31.769(2)	16.367(5)	13.7020(14)
c (Å)	22.870(2)	11.5480(8)	26.234(8)	17.5143(18)
β (deg)	105.696(2)	104.9970(10)		
V (Å^3)	4070.5(7)	3980.4(5)	8643(5)	4913.3(9)
Z	4	2	8	4
D_{calcd} (Mg/m^3)	1.298	1.299	1.307	1.266
μ (Mo Kα) (mm^{-1})	1.871	1.911	1.768	1.561
R1[a] (%) (all data)	3.28 (4.09)	4.66 (5.62)	5.39 (10.67)	4.27 (5.64)
wR2[b] (%) (all data)	7.47 (7.79)	8.40 (8.87)	7.90 (11.59)	8.11 (8.60)

[a] $R1 = \sum||F_o| - |F_c||/\sum |F_o|$ x 100. [b] $wR2 = [\sum w(F_o^2 - F_c^2)^2/\sum(w|F_o|^2)^2]^{1/2}$ x 100.

Table 6. Data Collection Parameters for **19**−**21**

	19	**20**	**21**
chemical formula	$C_{115}H_{98}Dy_2O_6Si_6$	$C_{70}H_{77}DyO_7Si_3$	$C_{69}H_{60}DyN_3O_3Si_3$
formula weight	2069.47	1277.09	1225.97
temp (K)	168(2)	168(2)	203(2)
space group	monoclinic	monoclinic	rhombohedral
	$P2(1)/n$	$P2(1)$	$R3m$
a (Å)	14.2341(15)	14.5532(15)	22.937(5)
b(Å)	15.4455(16)	16.4016(17)	22.937(5)
c (Å)	22.348(2)	14.8835(15)	12.123(5)
β (deg)	91.675(2)	115.6790(10)	
V (Å^3)	4911.2(9)	3201.8(6)	5523(3)
Z	2	2	3
D_{calcd} (Mg/m^3)	1.399	1.325	1.106
μ (Mo Kα) (mm^{-1})	1.639	1.275	1.104
R1[a] (%) (all data)	4.86(7.13)	2.79 (3.00)	6.40 (6.44)
wR2[b] (%) (all data)	8.95 (9.55)	6.33 (6.41)	16.19 (16.23)

[a] $R1 = \sum||F_o| - |F_c||/\sum|F_o|$ x 100. [b] $wR2 = [\sum w(F_o^2 - F_c^2)^2/\sum(w|F_o|^2)^2]^{1/2}$ x 100.

quality films based on their large exothermic decomposition pathways. Although there are numerous reports of $Ln(OR)_3$ in the literature, the variety of ligands, cations, and solvents used is diverse, and no systematic structural studies were readily available to allow us to select an appropriate precursor for our dopant investigation. Therefore, we synthesized and isolated a series of $Dy(OR)_3$ compounds that contained increasing sterically demanding ligands, including H−ONep, H−OBu^t, H−DMP, H−DIP, H−DBP, and H−TPS. In addition, we are interested in how the solvents used will affect their structure and isolated these species from tol, THF, and py when possible. The matrix used is shown in Table 7. Once developed, representative compounds were used to investigate the structural influences on the quality of the final PDyZT thin films.

Table 7. List of Structure Types Isolated for the Matrix of Ligands and Solvents Used to Explore $Dy(OR)_3$ Structures[a]

ligand	NH_3	tol	THF	py
ONep	hex[b]	**1** tetra (μ)	**2**[d] tri (μ and μ_3, 2)	**3** tri (μ and μ_3, 2)
OBu^t	—[c]	**4** tri (μ and μ_3)	**5** tri (μ and μ_3, 2)	**6** tri (μ and μ_3, 2)
DMP	**7** linear tri (2)	**8**[d] di (π, 0)	**9**[d] mono (3)	**10** mono (3)
DIP	**11** mono (2)	**12** di (π, 0)	**13** mono (2)	**14** mono (3)
DBP	**15** mono (1)	**16** mono (0)	**17** mono (1)	**18** mono (2)
TPS	—[c]	**19** di (μ)	**20** mono (3)	**21** mono (3)

[a] The nuclearity is listed, and the type of interaction used by the ligands to form the molecule and/or the number of solvent molecules bound are/is in parentheses. [b] hex = sodium contamination forms a poorly solved hexameric species. [c] — = never attempted. [d] No acceptable crystal solutions reported. Proposed structure presented in parentheses.

Synthesis. Several synthetic routes were undertaken in an attempt to generate this family of $Dy(OR)_3$ compounds: (a) ammoniacal shown in eq 1 and (b) amide−alcohol metathesis shown in eqs 2 and 3.

$$DyCl_3 + 3Na^0 + 3HOR \xrightarrow{NH_3(l)} Dy(OR)_3 + 3NaCl + {}^3/_2H_2 \quad (1)$$

$$DyCl_3 + 3LiN(SiMe_3)_2 \xrightarrow{hex} Dy(N(SiMe_3)_2)_3 + 3LiCl \quad (2)$$

$$Dy(N(SiMe_3)_2)_3 + 3HOR \xrightarrow{tol} Dy(OR)_3 + 3HN(SiMe_3)_2 \quad (3)$$

Initially, the established ammoniacal route to $Ln(OAr)_3$[5,10] was selected to generate the $Dy(OAr)_3$ derivatives (eq 1). X-ray quality crystals were isolated for **7**, **11**, and **15** which were solved as the ammonia derivatives, adding to this exclusive family of NH_3-bound Ln compounds.[5,10] Subsequent solvated species of these precursors were isolated by redissolution of the appropriate aryloxide in the desired solvent.

Attempting a similar reaction with the alkyl alkoxides using the ONep derivative led to a tetranuclear structure, **1** (Figure 1). However, attempts to crystallize the same powder from THF yielded **1a** (Figure 2), a highly disordered hexanuclear species that is not charge balanced. Two mechanisms are available to explain the structure of **1a**: (i) Na contamination is carried over from the original solution and was not observed upon crystallization from tol or (ii) the crystallization of **1** from THF can lead to an unusual crystalline material that adopts a disordered structure. Additional investigations to determine whether this is a contamination or a crystallization disorder issue are underway. However, because of the potential problems associated with the ammoniacal route, we undertook the alternative amide−alcohol synthetic route using $Dy(NR_2)_3$ (eq 3). Again, alkali metal contamination was observed.

$Dy(NR_2)_3$ was obtained from the reaction of $DyCl_3$ and 3 equiv of lithium amide.[11] A series of solvent washes, sublimations, and crystallizations led to the isolation of pure $Dy(NR_2)_3$ exhibiting a crystal structure that agreed with the literature report.[6] The use of pure starting material is critical to the isolation of high-quality crystals obtained in the next step. All subsequent reactions involved the systematic alcoholysis of $Dy(NR_2)_3$ in tol, as shown in eq 3. All further solvated species discussed below were isolated by dissolution of the product isolated from eq 1 or 3 in the appropriate solvent or through eq 3 performed in the same solvent.

X-ray Structures. A matrix of the various ligands and solvents used is shown in Table 7 with a summary of the structural types identified. The discussion that follows details the structures of the systematic family of $Dy(OR)_3$ compounds that have been synthesized and characterized.

***neo*-Pentoxide.** From eq 3, using tol as the solvent, a tetrameric structure was observed for **1** with a molecule of tol observed in the lattice. Compound **1** is the first $Dy(ONep)_3$ species isolated (Figure 1) wherein the central core was found to be identical to the previously reported ONep derivatives of La and Nd.[10] The Dy metal centers are arranged in a square shape interconnected by four bridging μ-ONep ligands and one terminal ONep ligand per metal center. Each of the Dy cations is five-coordinate, adopting a square-base-pyramidal (SBP) geometry. As noted for the La derivative, the ONep shows H-bonding, and additional

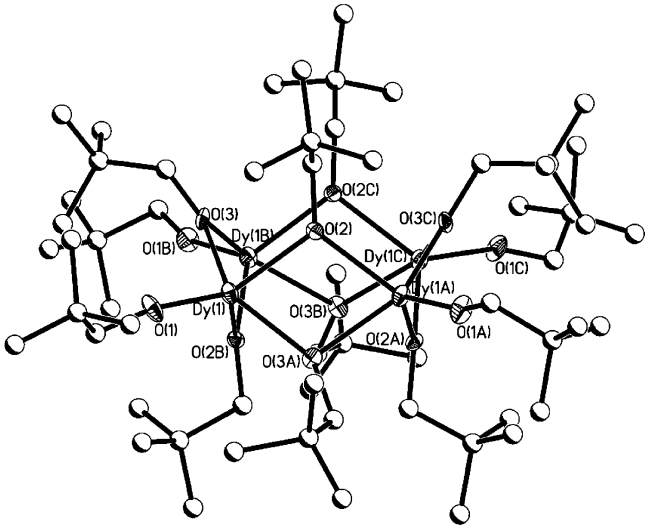

Figure 1. Plot of **1**. Heavy atoms are thermal ellipsoids drawn at the 30% level, and the carbon atoms are drawn in ball-and-stick format for clarity.

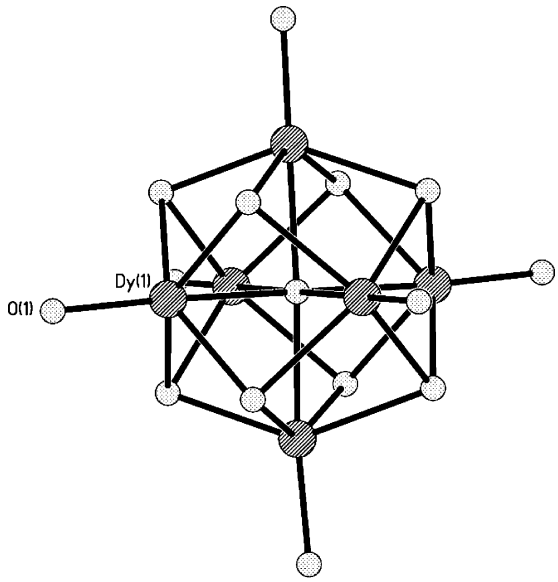

Figure 2. Ball-and-stick representation of **1a**. Carbon atoms are omitted for clarity.

work using this ligand and the remainder of the Ln cations has revealed a consistent trend.[12,13]

Attempts to isolate **1** from THF did not lead to the expected solvated adduct, but instead compound **1a** was solved. The central core of **1a** is shown in Figure 2 and exhibits a highly disordered "$M_6(O)(ONep)_{12}$" arrangement. This zwitterion-like core consists of four metal atoms arranged in a square, capped above and below by two additional cations. Each of the six metal atoms is bound to a μ_6-O , four μ_3-ONep, and one terminal ONep ligand. If all of the metals are considered Dy, an overall 4+ charge exists, and the model does not refine properly. Sodium atoms were introduced to compensate for the charge as Na contamination could have easily been introduced in the original reaction

(10) Barnhart, D. M.; Clark, D. L.; Gordon, J. C.; Huffman, J. C.; Vincent-Hollis, R. L.; Watkin, J. G.; Zwick, B. D. *Inorg. Chem.* **1994**, *33*, 3487.
(11) Bradley, D. C.; Mehrotra, R. C.; Gaur, D. P. *Metal Alkoxides*; Academic Press: New York, 1978.
(12) Boyle, T. J.; Ottley, L. M. Sandia National Laboratories, Albuquerque, New Mexico. Unpublished work; 2004.
(13) Boyle, T. J. Sandia National Laboratories, Albuquerque, New Mexico. Unpublished work; 2004.

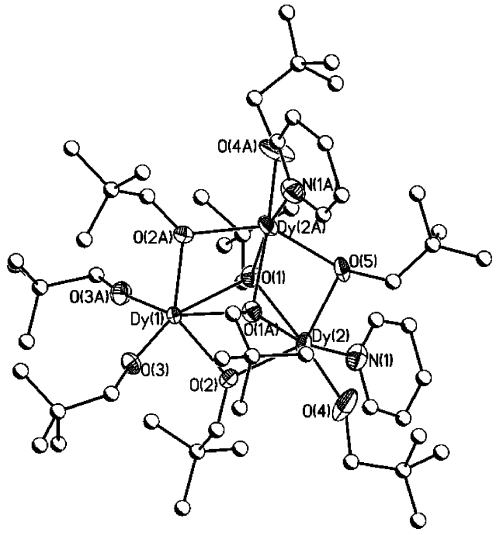

Figure 3. Plot of **3**. Heavy atoms are thermal ellipsoids drawn at the 30% level, and the carbon atoms are drawn in ball-and-stick format for clarity.

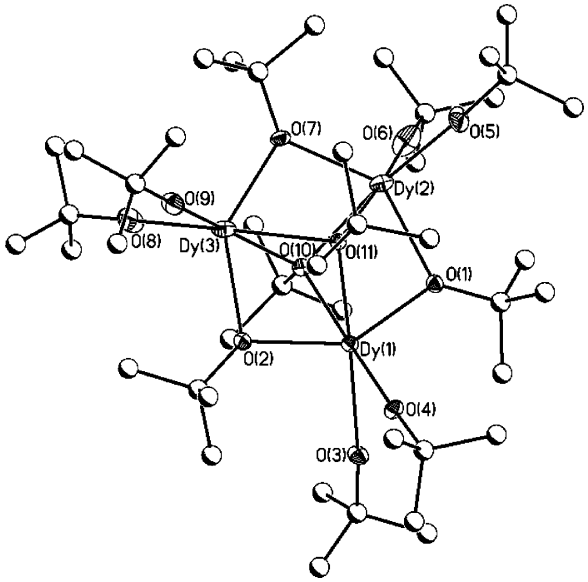

Figure 4. Plot of **4**. Heavy atoms are thermal ellipsoids drawn at the 30% level, and the carbon atoms are drawn in ball-and-stick format for clarity.

and carried through the tol wash. Again, refinement of any site as a full or partial Na atom occupation does not improve the refinement. Alternatively, the observed structure of **1a** might be a result of a partially rotated molecule that crystallizes in this orientation when THF is the solvent. Numerous attempts to grow higher-quality crystals did not improve the data or the subsequent model. Attempts to isolated this compound from the amide synthesis (eq 3) have not been successful (vide infra). However, **1a** is often observed in this and other $Ln(ONep)_3$ systems we are investigating with similar structural problems; therefore, the structure and subsequent parameters of **1a** are reported to avoid mischaracterization of **1**.

The amide−alcohol exchange route (eq 3) was then used to synthesize the ONep derivative in the presence of Lewis basic solvents (i.e., THF or py). For THF as the crystallization solvent, a fully substituted tetranuclear species was observed with THF in the lattice but not bound to the central core or the structure of **1a** (vide supra) was observed. Again, it is possible to have a Li atom as a contaminant from eq 2, and this led us to adopt the numerous purification steps for $Dy(NR_2)_3$. From pure $Dy(NR_2)_3$, we have not been successful in the isolation of a structure of the $Dy(ONep)_3$ with bound THF; however, upon switching to the stronger Lewis base py, a trinuclear complex was solved as **3** (Figure 3). It is assumed that **2** would be similar in structure to **3** based on the other species isolated in this and other[14,15] studies. For **3**, the Dy cations are interconnected by two triply bridging μ_3-ONep and three bridging μ-ONep ligands. Two of the Dy metal centers complete their distorted octahedral (O_h) geometry by binding one terminal ONep ligand and a solvent molecule, whereas the third Dy uses two ONep ligands. The structure type observed here is similar to several other lanthanide alkoxide trinuclear species previously reported but the ligand sets of those compounds were typically OBu^t or fluorinated species.[14−19] It is of note that only two previous $Ln(OR)_3$ structures have been reported with coordinated py as the solvent molecules, $[Nd(\mu\text{-}OR)(OR)_2(py)]_2$ where OR = $OCH(CH(Me_2)_2)_2$[20] or $OC_6H_2Me_3$-2,4,6.[21]

***tert*-Butoxide.** Increasing the steric bulk of the pendant alkoxide chain from ONep to OBu^t reduced the nuclearity from the tetramer to a trimer when crystallized from tol. The trimer of **4** (Figure 4) adopts an O_h arrangement using two μ_3-OBu^t, three μ-OBu^t, and six terminal OBu^t. Because of charge balance, two free $HOBu^t$ are necessarily bound to the molecule. This structure is consistent with the $[La(OBu^t)_3]_3(HOBu^t)_2$ structure reported by Bradley and coworkers.[16] Additional studies have shown that tetranuclear species of Ln species with OBu^t as the ligand can be isolated if there is no Lewis basic species present;[12] however, this was not realized with this system. Crystallization from THF yielded simple substitution of the bound $HOBu^t$ with THF to form **5**, shown in Figure 5, which is isostructural with the $Nd(OBu^t)_3$ derivatives isolated from THF.[14,15] The py adduct (**6** shown in Figure 6) exhibits constructs similar to those in **5** with the THF ligands replaced by py.

2,6-Dimethyl Phenoxide. As can be observed from the increase in steric bulk from ONep to OBu^t, a decrease in nuclearity was observed. Therefore, it was of interest to determine the effect of di-ortho-substituted phenoxides on the final structure, given that, from previous studies,[22−24] we

(14) Gromada, J.; Chenal, T.; Morteux, A.; Ziller, J. W.; Leising, F. *Chem. Commun.* **2000**, 2183.
(15) Gromada, J.; Mortreux, A.; Chenal, T.; Ziller, J. W.; Leising, F. *Chem.-Eur. J.* **2002**, *8*, 3773.
(16) Bradley, D. C.; Chudzynska, H.; Hursthouse, M. B.; Motevalli, M. *Polyhedron* **1991**, *10*, 1049−1059.
(17) Bradley, D. C.; Chudzynska, H.; Hursthouse, M. B.; Motevalli, M.; Hammond, M. E.; Ruowen, W. *Polyhedron* **1992**, *11*, 375−379.
(18) Bradley, D. C.; Chudzynska, H.; Hursthouse, M. B.; Motevalli, M.; Wu, R. W. *Polyhedron* **1993**, *12*, 2955−2960.
(19) Gun'ko, Y. K.; Elliot, S. D.; Hitchcock, P. B.; Lappert, M. F. *J. Chem. Soc., Dalton Trans.* **2002**, 1853.
(20) Barnhart, D. M.; Clark, D. L.; Huffman, J. C.; Vincent, R. L. *Inorg. Chem.* **1993**, *32*, 4077.
(21) Giesbrecht, G. R.; Gordon, J. C.; Clark, D. L.; Scott, B. L. *Inorg. Chem.* **2002**, *41*, 6372.
(22) Boyle, T. J.; Andrews, N. L.; Rodriguez, M. A.; Campana, C.; Yiu, T. *Inorg. Chem.* **2003**, *42*, 5357−5366.

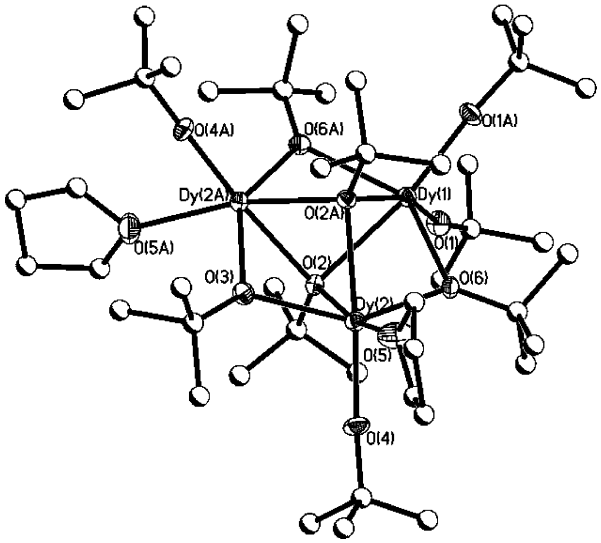

Figure 5. Plot of **5**. Heavy atoms are thermal ellipsoids drawn at the 30% level, and the carbon atoms are drawn in ball-and-stick format for clarity.

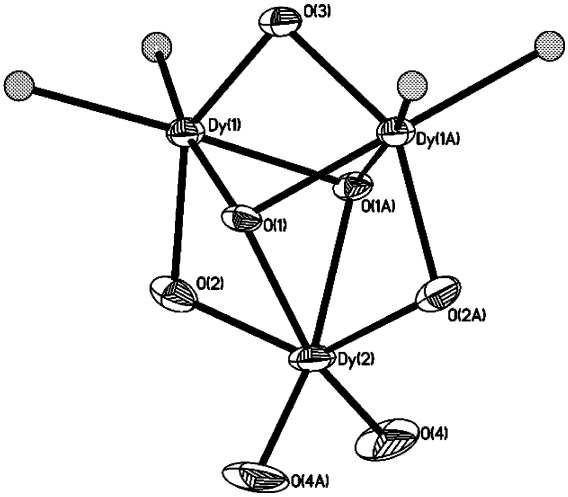

Figure 6. Plot of the core of **6**. Heavy atoms of the trinuclear species are thermal ellipsoids drawn at the 30% level. The disorder in the O of the terminal OBu^t and N of the py ligands leads to very large thermal ellipsoids, so these atoms are represented as simple balls and left unassigned.

have found that the steric bulk of these ligands plays a pivotal role in the final nuclearity. It was discerned that the ammoniacal synthetic route using aryloxides produced high-quality crystals that did not contain any Na contamination. This was attributed to the increased steric bulk preventing the need for filling of open coordination sites; however, ammonia adducts are easily isolated. In the literature, only a few ammonia lanthanide adducts have been reported,[5,17,25−29] including $[Pr(OC(CF_3)_3(NH_3)_2]_2$[17,26] and $La(DIP)_3(NH_3)_3$.[5]

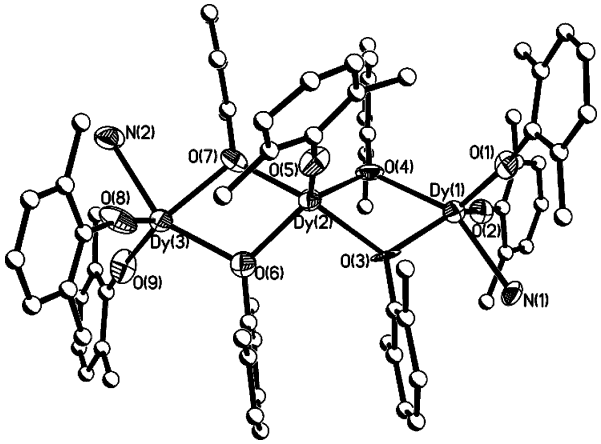

Figure 7. Plot of **7**. Heavy atoms are thermal ellipsoids drawn at the 30% level, and the carbon atoms are drawn in ball-and-stick format for clarity.

The DMP−NH_3 adduct **7** is shown in Figure 7 and was isolated as a linear trinuclear species with each metal center adopting an SBP geometry. Surprisingly, only one other Ln structure had a linear trinuclear geometry, $Eu[(\mu\text{-DMP})_3Eu(THF)_3]_2$.[30] For **7**, the central Dy uses four bridging DMP and one terminal DMP ligands to form a trigonal-bipyramidal (TBP) geometry. The terminal TBP-coordinated Dy atoms link to two μ-DMPs, two terminal DMPs, and one NH_3 group. This is in contrast to the Eu species discussed previously, which has three bridging and three terminal THF ligands. The variation in bound solvent is most likely explained by the reduction in the Dy cation size.[31] The balance between the steric bulk of the DMP ligand combined with the coordination of the Lewis basicity of the NH_3 must be too large to form the trinuclear arrangement[14−19] but not small enough to allow the dinuclear[17,20,21,26] arrangement noted for most lanthanide species.

Removal of the NH_3 through refluxing of a reaction mixture of **7** in tol led to the isolation of **8**. X-ray quality crystals could not be isolated for this powder. From the literature, there are ∼20 lanthanide structures that use an aryloxide with two methyl groups present in the ortho position;[32] however, all of these compounds include coordinated solvents, alternative ligands, or additional metal centers. These variations tend to fill coordination sites limiting the size of the molecules. It has been shown that a reduction in the number of coordination sites by solvent molecules leads to larger clusters {i.e., $Y(DMP)_3(THF)_3$ versus $[Y(DMP)_3(THF)]_2$}.[33] Therefore, although it is difficult to predict the structure of **8** given that no homoleptic $Ln(DMP)_3$ without solvent coordination are available, two structures have been proposed on the basis of available data. One structure might be similar to **7** with the NH_3 removed

(23) Boyle, T. J.; Pedrotty, D. M.; Alam, T. M.; Vick, S. C.; Rodriguez, M. A. *Inorg. Chem.* **2000**, *39*, 5133−5146.
(24) Boyle, T. J.; Rodriguez, M. A.; Ingersoll, D.; Headley, T. J.; Bunge, S. D.; Pedrotty, D. M.; De'Angeli, S. M.; Vick, S. C.; Fan, H. *Chem. Mater.* **2002**, *15*, 3903.
(25) Berg, D. J.; Anderson, R. A.; Zalkin, A. *Organometallics* **1988**, *7*, 1858.
(26) Bradley, D. C.; Chudzynska, H.; Hursthouse, M. B.; Motevalli, M. *Polyhedron* **1994**, *13*, 7−14.
(27) Wang, K.-G.; Stevens, E. D.; Nolan, S. P. *Organometallics* **1992**, *11*, 1101.
(28) Wayda, A. L.; Dye, J. l.; Rogers, R. D. *Organometallics* **1984**, *3*, 1605.
(29) Zalkin, A.; Henly, T. J.; Andersen, R. A. *Acta Crystallogr. C: Cryst. Struct. Commun.* **1987**, *43*, 233.
(30) Evans, W. J.; Greci, M. A.; Ziller, J. W. *Inorg. Chem.* **2000**, *39*, 3213.
(31) Shannon, R. D. *Acta Crystallogr.* **1976**, *A32*, 751.
(32) Twenty compounds were identified with three DMP ligands and any lanthanide atom (La and Y) using the Cambridge Crystallographic Data Centre, 12 Union Road, Cambridge CB2 1EZ, United Kingdom, www.ccdc.cam.ac.uk, which was searched using ConQuest v 5.25 (Apr 2004).
(33) Evans, W. J.; Olofson, J. M.; Ziller, J. W. *Inorg. Chem.* **1989**, *28*, 4308.

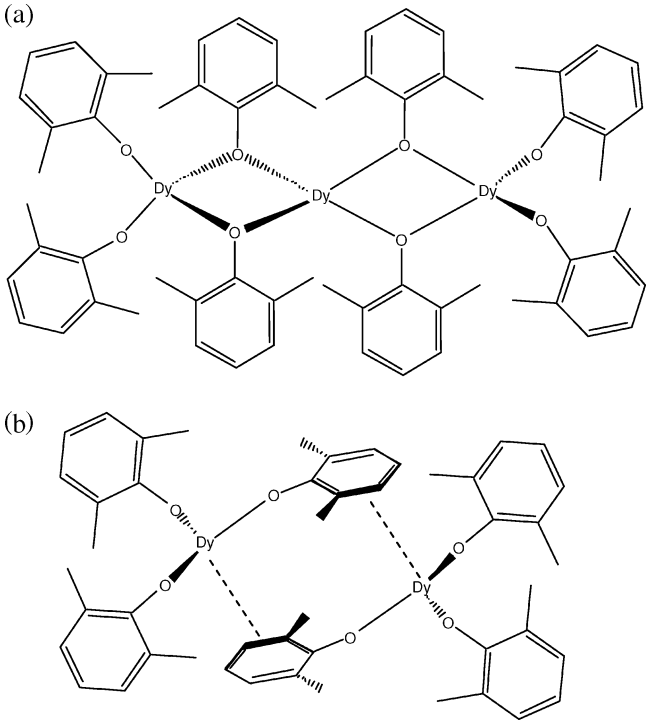

Figure 8. Schematic representation of proposed structures of **8**: (a) trinuclear species, (b) π-bound dinuclear species.

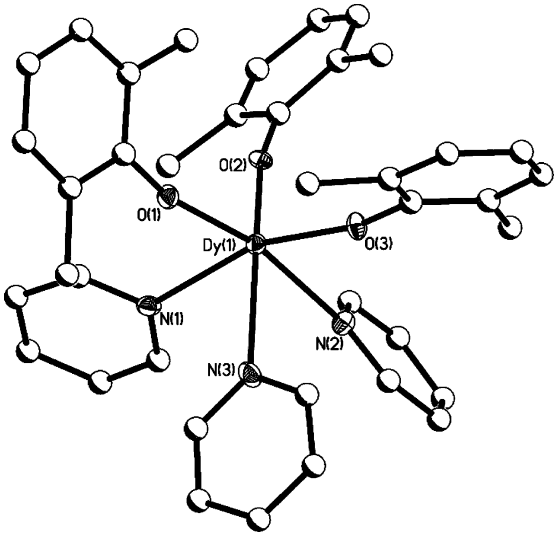

Figure 9. Plot of **10**. Heavy atoms are thermal ellipsoids drawn at the 30% level, and the carbon atoms are drawn in ball-and-stick format for clarity.

as shown in Figure 8a. The lack of a Lewis base coupled with the steric bulk of the DMP ligands stabilizing the open coordination sites could lead to this type of structure; however, there are no representative trinuclear structures in the literature. The other structure might be similar to that of the La(DIP)$_3$ adduct and is schematically shown in Figure 8b.[5] Because the coordination spheres of the Dy would be filled and the larger structure exists, this is the preferred structural arrangement. Further attempts to crystallize **8** from THF also did not yield X-ray quality crystals either. On the basis of literature reports,[33] however, the powder was assumed to be the monomer **9** and similar to what was observed for the py adduct that was crystallographically

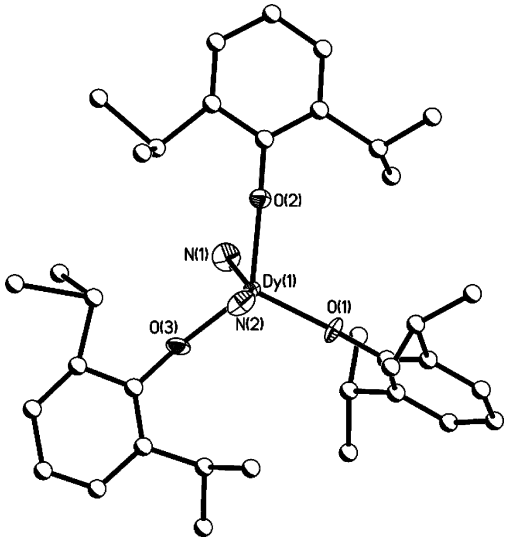

Figure 10. Plot of **11**. Heavy atoms are thermal ellipsoids drawn at the 30% level, and the carbon atoms are drawn in ball-and-stick format for clarity.

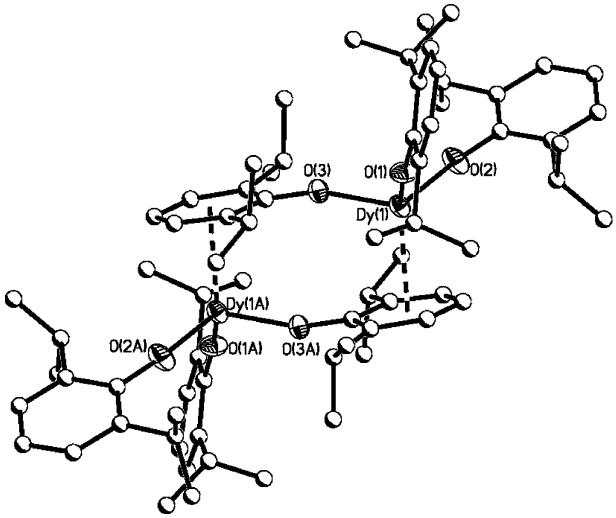

Figure 11. Plot of **12**. Heavy atoms are thermal ellipsoids drawn at the 30% level, and the carbon atoms are drawn in ball-and-stick format for clarity.

characterized as **10** (Figure 9). Three solvent molecules bind to form a mononuclear O_h-arranged species with an additional molecule of solvent in the lattice for each.

2,6-Diisopropyl Phenoxide. Using the increased steric bulk of the DIP ligand in the ammoniacal synthesis, a monomer, **11**, coordinated by two NH_3 molecules was isolated. A plot of **11** is shown in Figure 10. Several DIP lanthanide derivatives have been isolated, the majority of which are mononuclear species through the coordination of solvents.[5,10,34,35] The distorted TBP geometry is unusual given that there appears to be room to coordinate another NH_3 molecule to form an O_h arrangement, as was noted for the La(DIP)$_3$ derivative that bound four NH_3 molecules.[5] Again, the smaller size of the Dy cation in comparison to the La

(34) Xie, Z. W.; Wang, S. W.; Zhou, Z. Y.; Mak, T. C. W. *Organometallics* **1998** *17*, 1907.
(35) Clark, D. L.; Gordon, J. C.; Watkin, J. G.; Huffman, J. C.; Zwick, B. D. *Polyhedron* **1996**, *15*, 2279.

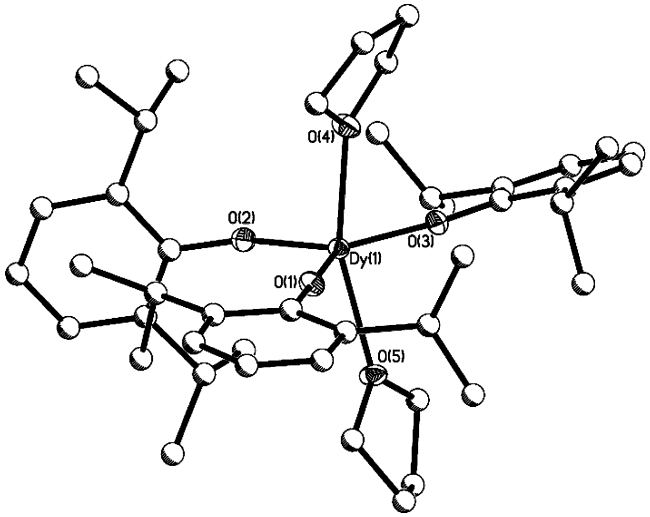

Figure 12. Plot of **13**. Heavy atoms are thermal ellipsoids drawn at the 30% level, and the carbon atoms are drawn in ball-and-stick format for clarity.

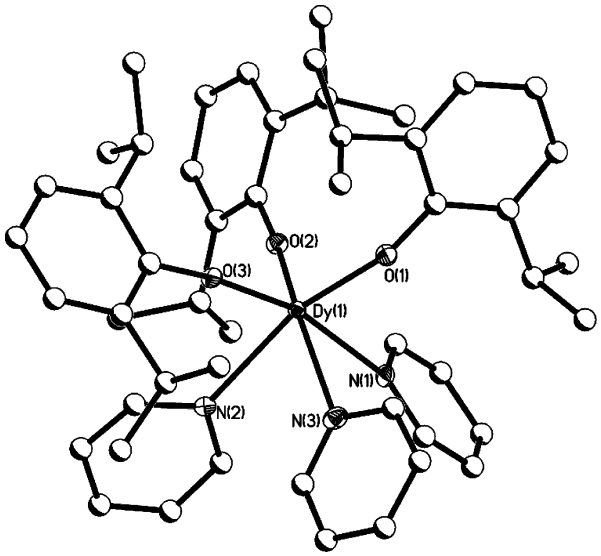

Figure 13. Plot of **14**. Heavy atoms are thermal ellipsoids drawn at the 30% level, and the carbon atoms are drawn in ball-and-stick format for clarity.

cation must account for the variation.[31] Removal of the NH_3 from **11** leads to the isolation of **12** (Figure 11), which adopts a structure where the π-ring of the DMP coordinates to the Dy, identical to what was observed for [La(η-DIP)(DIP)$_2$]$_2$.[5] Lewis basic solvents reduce this interaction, forming the TBP-coordinate monomer **13** with two axial THF solvent molecules and the O_h-bound monomer **14** with three coordinated py molecules, similar to what was noted for **10**. Figures 12 and 13 are plots of **13** and **14**, respectively.

2,6-Di-*tert*-butyl Phenoxide. Using the most sterically hindering ligand in our study (DBP), we isolated several monomers, **15**−**18** (Figures 14−17, respectively). In the presence of a Lewis base, T_d-bound Dy ions were isolated for NH_3(l) (**15**) or THF (**17**) adducts, whereas a TBP arrangement was noted for **18**, which uses two py molecules. This variation is most likely a representation of the stronger Lewis basicity of py. A monomer was also isolated for the reaction product of eq 3 run in tol. The Dy atom of

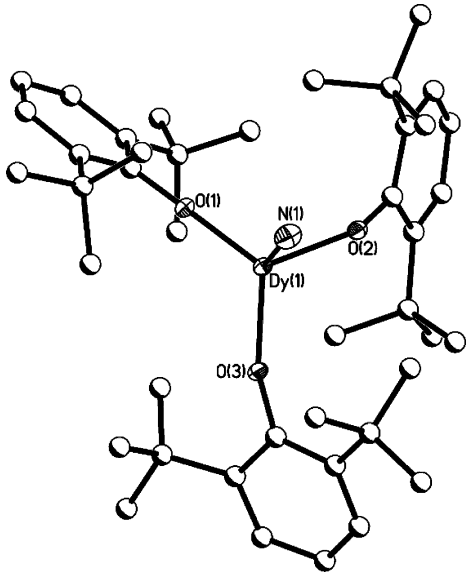

Figure 14. Plot of **15**. Heavy atoms are thermal ellipsoids drawn at the 30% level, and the carbon atoms are drawn in ball-and-stick format for clarity.

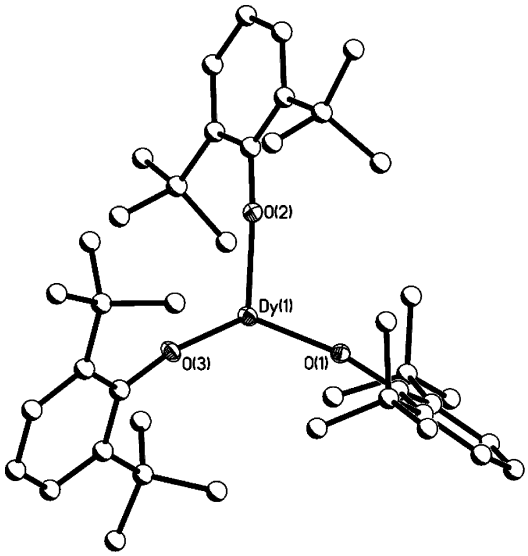

Figure 15. Plot of **16**. Heavy atoms are thermal ellipsoids drawn at the 30% level, and the carbon atoms are drawn in ball-and-stick format for clarity.

compound **16** adopts a trigonal geometry with no interaction between the metal centers and the pendant aryl chains, as noted for La. This is most likely due to the reduction in cation size.[31] Literature studies also show that other Ln−DBP-like derivatives adopt mononuclear structures for solvated and dinuclear for unsolvated compounds.[36−38] The latter dinuclear species was for the smaller Yb cation.

Triphenylsiloxide. We were also interested in how a siloxane would affect structural aspects. Using the TPS ligand, we isolated the dinuclear complex **19** from tol, which contains T_d-bound Dy atoms consisting of two μ-TPS and

(36) Stecher, H. A.; Sen, A.; Rheingold, A. L. *Inorg. Chem.* **1988**, *27*, 1130.
(37) van den Hende, J. R.; Hitchcock, P. B.; Holmes, S. A.; Lappert, M. F. *J. Chem Soc., Dalton Trans.* **1995**, 1435.
(38) van den Hende, J. R.; Hitchcock, P. B.; Lappert, M. F. *Chem. Commun.* **1994**, 1413.

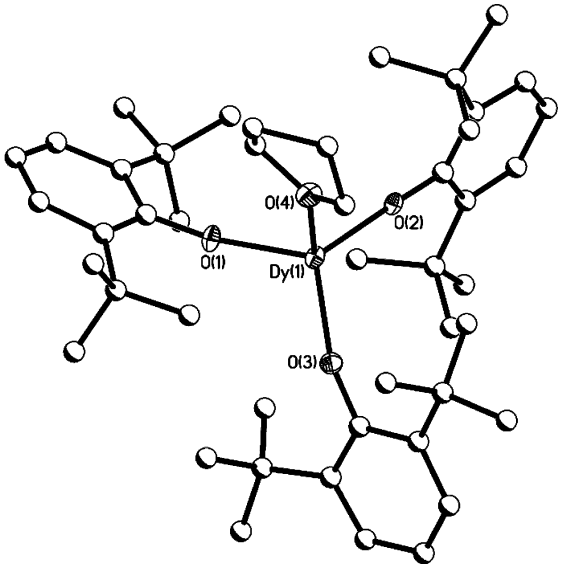

Figure 16. Plot of **17**. Heavy atoms are thermal ellipsoids drawn at the 30% level, and the carbon atoms are drawn in ball-and-stick format for clarity.

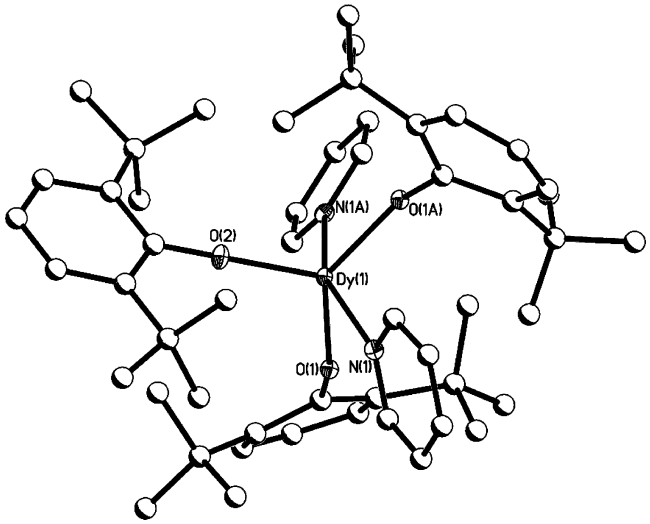

Figure 17. Plot of **18**. Heavy atoms are thermal ellipsoids drawn at the 30% level, and the carbon atoms are drawn in ball-and-stick format for clarity.

two terminal ligands, similar to the constructs of the Ce adduct.[39] From THF, the monomeric species **20** was isolated using three THF molecules and three TPS ligands to form the O_h environment of the Dy cation. This is consistent with the La,[40] Ce,[41] Pr,[41] and Sm[42] adducts. From py, a geometry similar to that noted for THF was observed for **21** with py replacing the THF molecules. Plots of the TPS-ligated species **19**−**21** are shown in Figure 18−20, respectively.

In summary, for the nonsolvated $Dy(OR)_3$ compounds characterized, the structures range from tetra- to tri- to di-

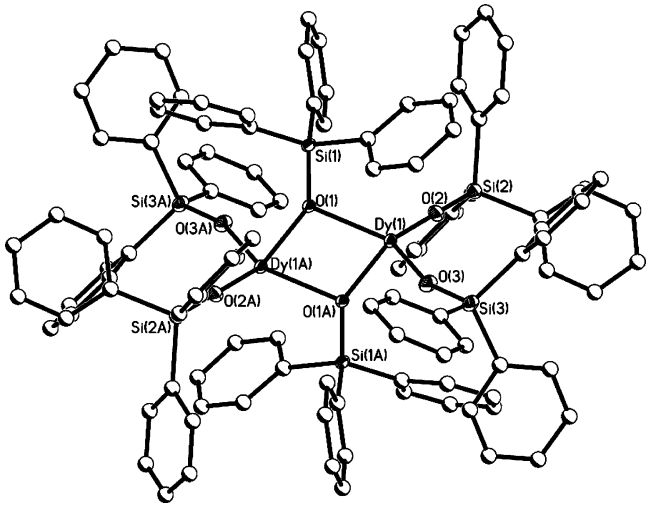

Figure 18. Plot of **19**. Heavy atoms are thermal ellipsoids drawn at the 30% level, and the carbon atoms are drawn in ball-and-stick format for clarity.

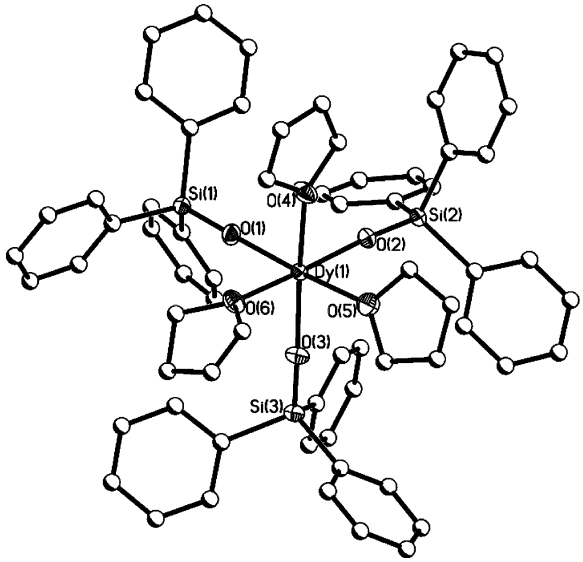

Figure 19. Plot of **20**. Heavy atoms are thermal ellipsoids drawn at the 30% level, and the carbon atoms are drawn in ball-and-stick format for clarity.

(π-bound or μ-OR) to mononuclear species as the steric bulk is increased. In general, as the reduction in the amount of steric bulk around the metal center is increased, the nuclearity decreases. For the DIP aryloxides, the rings of the ligand can act as a bridge because they are located relatively close to the metal center, but this is not the case for the DBP or the TPS ligands. For the former, the ortho substituents must block any potential interactions, whereas for the latter, only bridging through the oxygen occurs since the rings are too far removed to induce the same interaction. All polynuclear species are easily disrupted through the introduction of solvents where the ability to displace another solvent follows the Lewis base strength order of NH_3 < THF ≪ py. Again, the degree of bound solvent is directly influenced by the steric bulk of the ligand present. The metrical data of **1**−**21** are self-consistent and in-line with the values observed for the other lanthanide species.[2−6,10,14−21,25−29,34,35,42−44]

(39) Evans, W. J.; Golden, R. E.; Ziller, J. W. *Inorg. Chem.* **1991**, *30*, 4963.
(40) McGeary, M. J.; Coan, P. S.; Folting, K.; Streib, W. E.; Caulton, K. G. *Inorg. Chem.* **1991**, *30*, 1991.
(41) Gradeff, P. S.; Yunlu, K.; Deming, T. J.; Olofson, J. M.; Doedens, R. J.; Evans, W. J. *Inorg. Chem.* **1990**, *29*, 420.
(42) Xie, Z.; Chui, K.; Yang, Q.; Mak, T. C. W.; Sun, J. *Organometallics* **1998** *17*, 3937.

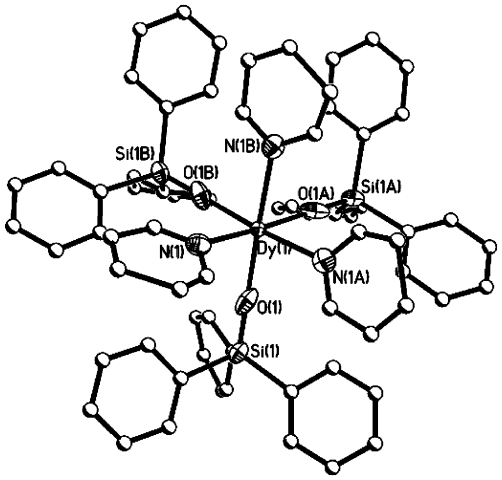

Figure 20. Plot of **21**. Heavy atoms are thermal ellipsoids drawn at the 30% level, and the carbon atoms are drawn in ball-and-stick format for clarity.

Bulk Evaluation. Because of the paramagnetic nature of the Dy compounds, NMR (solution and solid state) spectroscopic data were not available. FTIR data were collected for **1**−**21** using a KBr pellet press. These all show the requisite stretches for the ligands used minus the OH stretch (except for **4**) and the appropriate solvent stretches and bends. The Dy−O stretch could not be discerned from the numerous peaks in the fingerprint region. Elemental analyses were also collected for **1**−**21**. The analyses appear to be in good agreement with the crystal structures observed for the majority of samples. Any variations are typically associated with solvated species wherein preferential loss of bound solvent or solvent molecules trapped in the lattice occurs.

Film Production. Approximately 0.4 M precursor solutions to $PbZr_{0.3}Ti_{0.7}O_3$ (PZT 30/70) were generated as described in the Experimental Section, following the established BRP process.[1,8,9] The amount of Dy doping in the PZT 30/70 films was selected to be 4%, based on the highest levels readily obtainable without secondary phase formation, as previously noted for PLaZT studies. Because of the high solubility of **12**, this compound was used as the dopant for the PDyZT (4/30/70). Films spin-coated from this solution were visually high in quality with few visible defects observed and were found to contain a single-phase, tetragonal perovskite structure with lattice parameters $a = 3.99$ Å and $c = 4.12$ Å with an approximate unit cell volume of ∼65.7 Å^3. Diffraction patterns of the PDyZT perovskite phase displayed a preference for the (111) out-of-plane orientation; however, other (*hkl*) values were also observed. These results are consistent with data collected on previous specimens.[1,8]

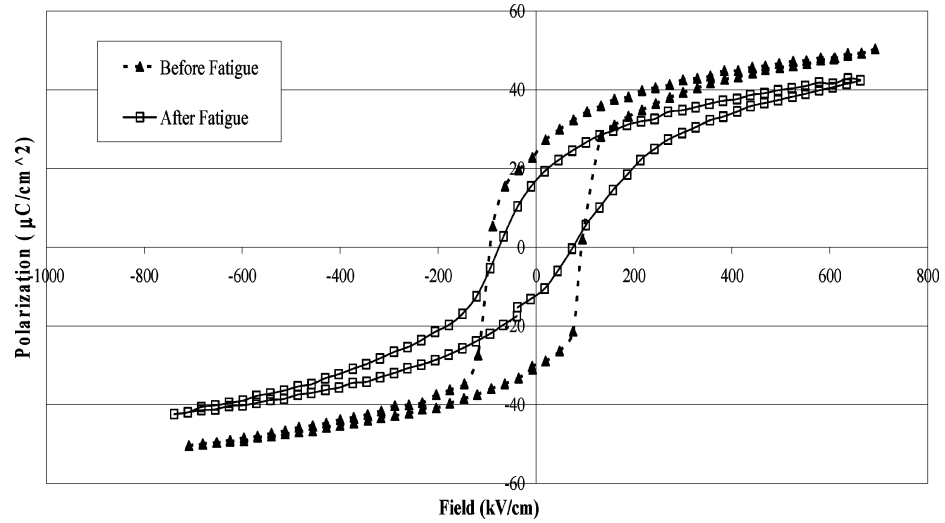

Figure 21. Hysteresis loops of PZT (30/70) (a) before (▲) and (b) after (□) fatigue testing.

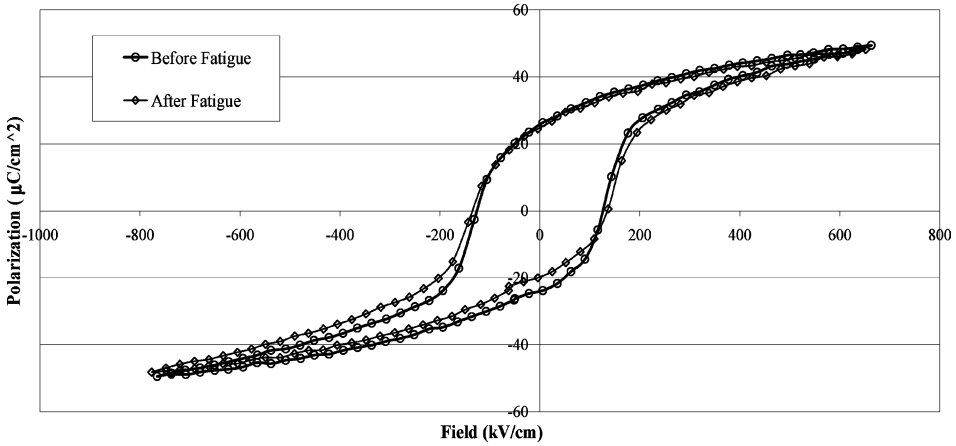

Figure 22. Hysteresis loops of PDyZT (4/30/70) (a) before (○) and (b) after (◇) fatigue testing.

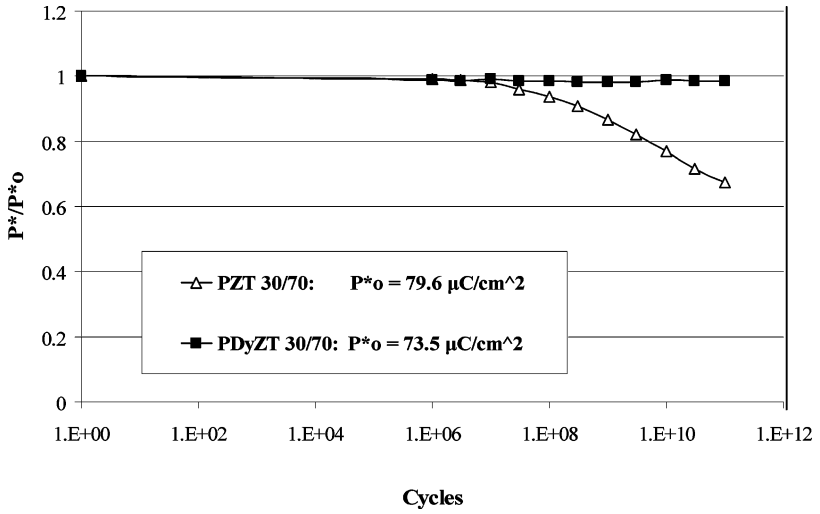

Figure 23. Plot of P^* versus cycles for PZT and PDyZT.

The hysteresis loops prior to fatigue of PZT and PDyZT are shown in Figures 21a and 22a, respectively. For PZT, these loops were square and narrow with spontaneous polarization (P_r) = 24 μC/cm^2, coercive field (E_c) = 93 kV/cm, $\epsilon' = 396$, and tan $\delta = 0.007$ (10 kHz, 100 mV). These are reasonable values in comparison to our previous literature reports.[1,8,9] For the PDyZT films, comparable values were obtained: $P_r = 26$ μC/cm^2, $E_c = 126$ kV/cm, $\epsilon' = 343$, and tan $\delta = 0.009$ (10 kHz, 100 mV). Although the films appear to be very similar in initial properties, the fatigue behavior was discovered to be substantially different between the two films, presumably because of the inclusion of the amphoteric Dy cations. It is believed that amphoteric dopants in perovskites can occupy either the Pb or Zr/Ti site, thereby suppressing the concentration of nonstoichiometry-related oxygen vacancies, which are associated with ferroelectric fatigue.[1]

The hysteresis loops after fatigue testing of PZT and PDyZT are shown in Figures 21b and 22b, respectively. A plot of the switched polarization (P^*) versus number of ferroelectric switching cycles is shown in Figure 23. In contrast to the PZT film ,which fatigues around 10^7 cycles (a substantial improvement over standard films, which typically fatigue around 10^5 cycles at 250 kV/cm),[1] the PDyZT films showed almost no fatigue for up to 10^{11} cycles. This is an impressive display of resistance to fatigue given that the test was run at a field of 700 kV/cm, or roughly 2.5 times higher than the applied field used for the undoped PZT.[1] This resistance to fatigue due to Dy doping suggests applications for such films in smart card and other nonvolatile memory applications, where a 10-year lifetime might consist of 10^{13} cycles. Resistance to voltage degradation of switching properties might also be of interest for piezoelectric sensor or optical switch applications, for which a long lifetime and large number of polarization reversals can be required.

Summary and Conclusions

We have developed a comprehensive family of $Dy(OR)_3$ compounds (**1**−**21**) synthesized by an amide−alcohol exchange or an ammoniacal preparative route. The final structures of the isolated products exhibit a variety of arrangements depending on the steric bulk of the ligands introduced and the solvents used for crystallization. In general, the smaller ligands (i.e., ONep or OBu^t) led to oligomers such as tetramers and trimers, whereas larger ligands (aryloxides or siloxides) led to dimers and monomers. The construction of the ligand allows for either preferential bridging or π-bonded bridging. For the monomeric species, the coordination around the Dy metal center was controlled by the amount of solvent bound, which was directly related to the solvent's Lewis basic strength. Compound **12** was chosen as the dopant, and the resultant $Pb_{0.94}Dy_{0.04}Zr_{0.30}Ti_{0.70}$ (4/30/70) films were found to be substantially improved in terms of fatigue in comparison to the undoped films. The development of a number of new Dy precursors is hoped to enable larger-scale studies of the exact mechanism of this effect.

Acknowledgment. For support of this research, the authors thank the Office of Basic Energy Sciences of the Department of Energy and the United States Department of Energy. Sandia is a multiprogram laboratory operated by Sandia Corporation, a Lockheed Martin Company, for the United States Department of Energy under Contract DE-AC04-94AL85000.

Supporting Information Available: X-ray crystallographic files in CIF format for the structures **1**−**21** (not available for **2**, **8**, and **9**). This material is available free of charge via the Internet at http://pubs.acs.org.

IC048550B

(43) Deacon, G. B.; Feng, T.; Nickel, S.; Ogden, M. I.; White, A. H. *Aust. J. Chem.* **1992**, *45*, 1992.
(44) Giesbrecht, G. R.; Gordon, J. C.; Brady, J. T.; Clark, D. L.; Keogh, D. W.; Michalczyk, R.; Scott, B. L.; Watkin, J. G. *Eur. J. Inorg. Chem.* **2002**, 723.